

# Influence of heating rate on optical properties of Nd:YAG laser ceramic

Wenbin Liu<sup>a,b</sup>, Benxue Jiang<sup>b</sup>, Wenxin Zhang<sup>b</sup>, Jiang Li<sup>b</sup>, Jun Zhou<sup>b</sup>,  
Di Zhang<sup>a</sup>, Yubai Pan<sup>b,\*</sup>, Jingkun Guo<sup>b</sup>

<sup>a</sup> State Key Laboratory of Metal Matrix Composites, Shanghai Jiao Tong University, 800 Dongchuan Road, Shanghai 200240, PR China

<sup>b</sup> State Key Laboratory of Transparent Opto-functional Inorganic Materials, Shanghai Institute of Ceramics, Chinese Academy of Sciences, 1295 Dingxi Road, Shanghai 200050, PR China

Received 27 January 2010; received in revised form 3 March 2010; accepted 7 May 2010

Available online 17 June 2010

## Abstract

Using commercial  $\alpha$ - $\text{Al}_2\text{O}_3$ ,  $\text{Y}_2\text{O}_3$  and  $\text{Nd}_2\text{O}_3$  as raw materials, 0.8 at% Nd:YAG ceramics were fabricated by solid-state reaction and vacuum sintering technology, with tetraethoxysilane (TEOS) as sintering aid. The Nd:YAG ceramics were obtained by sintering at 1750 °C for 20 h under vacuum. The sintering process with different heating rate of the Nd:YAG ceramics have been studied during the present work. The grain sizes, pores and secondary phase amounts increased versus increasing the heating rate. The optical properties of the Nd:YAG ceramics were closely related to the microstructures of the specimens. The lasing performance of the Nd:YAG ceramics changed drastically with change in pores and secondary phase amounts.

© 2010 Elsevier Ltd and Techna Group S.r.l. All rights reserved.

**Keywords:** C. Optical properties; Nd:YAG ceramics; Heating rate; Microstructure

## 1. Introduction

Since 1995, polycrystalline YAG ceramic laser materials have received much attention because the optical quality has been improved greatly and highly efficient laser oscillations could be obtained [1,2]. Low duration and low cost of manufacturing, absence of severe limitation in size and geometry make the transparent yttrium aluminum garnet ( $\text{Y}_3\text{Al}_5\text{O}_{12}$ :YAG) ceramics attractive with comparison to single crystals [3–5]. Laser ceramic permits design flexibility (sandwich structures, etc.), and possibility of high power laser, development of high output laser using microchip and the laser technologies, which is extremely important, but cannot be realized in conventional single crystal materials [6]. But it was reported in previous papers that the optical quality of the conventional transparent ceramics was a little inferior to that of single crystal material, because of the residual pores and grain boundaries in the ceramics act as optical scattering centers [7–10,3]. To decrease optical loss, it is extremely important to fabricate super full dense ceramics with pore-free structure and clean grain boundaries. The properties of

the Nd:YAG ceramics are clearly related to the final microstructure. In the Nd:YAG ceramics sintering procedure, the average grain size of the ceramics mainly depends on the parameters of sintering [9,10]. As a result, sintering mechanism study of transparent ceramics has become a hot research topic [3], in terms of decreasing of pores and secondary phases.

Besides the sintering temperature and holding time, the heating rate has the same important impact on the grain growth and the composition diffusion, So in this paper, we discuss on the sintering process with different heating rate of Nd:YAG ceramics. The microstructure and optical properties of the Nd:YAG ceramics were studied in this paper.

## 2. Experimental procedure

High-purity  $\alpha$ - $\text{Al}_2\text{O}_3$  (99.99%),  $\text{Y}_2\text{O}_3$  (99.99%), and  $\text{Nd}_2\text{O}_3$  (99.99%) were used as starting materials. These powders were blended with the stoichiometric ratio of 0.8 at% Nd:YAG ceramics with the high-purity  $\text{Al}_2\text{O}_3$  balls for 10 h in ethanol, with tetraethylorthosilicate (TEOS) as sintering aid. Then the ethanol solvent was removed by drying the milled slurry at 80 °C for 24 h in oven. The dried powder mixture was ground and sieved through 200-mesh screen, dry-pressed under 100 MPa into  $\text{Ø}100 \times 7 \text{ mm}^2$  disks and finally cold-isostatically

\* Corresponding author. Tel.: +86 21 52412820; fax: +86 21 52413903.

E-mail address: [ybpan@mail.sic.ac.cn](mailto:ybpan@mail.sic.ac.cn) (Y. Pan).

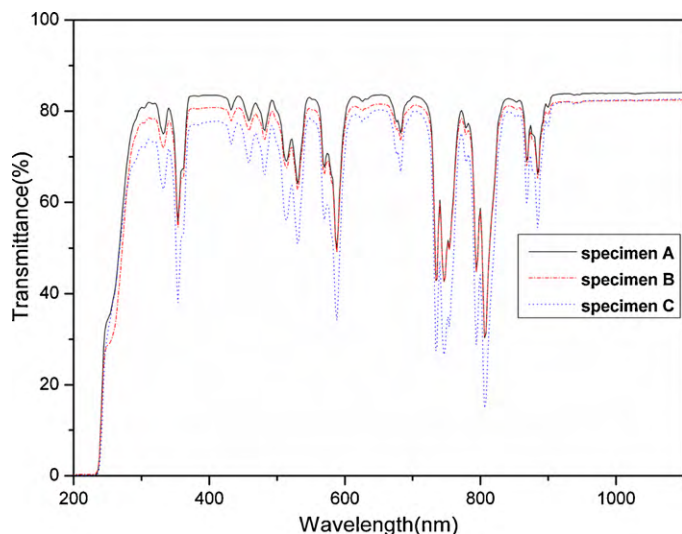


Fig. 1. Optical transmittance of specimens A, B and C ( $\varnothing 80 \times 5.5 \text{ mm}^2$ ).

pressed under 250 MPa. Green compacts were sintered at 1750 °C for 20 h in a tungsten mesh-heated vacuum furnace under vacuum ( $1.0 \times 10^{-3} \text{ Pa}$ ) with different heating rates: 1 °C/min, 2 °C/min and 5 °C/min, named as specimen A, specimen B and specimen C, respectively. After sintering, the specimens were annealed at 1450 °C for 20 h in air.

Mirror-polished samples ( $\varnothing 80 \times 5.5 \text{ mm}^2$ ) on both surfaces were used to measure optical transmittance (Model U-2800 Spectrophotometer, Hitachi, Japan). The phase compositions of specimens were identified by X-ray diffraction (XRD, Model

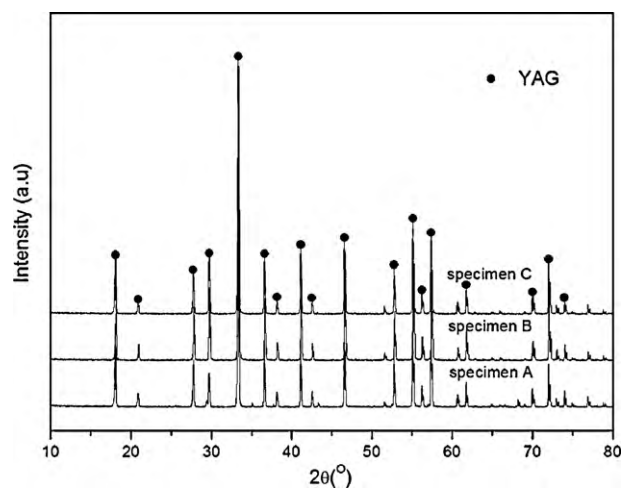


Fig. 2. XRD patterns of specimens A, B and C.

D/MAX-2550V, Rigaku, Japan). Microstructures of the thermal etched surfaces of the Nd:YAG ceramics were observed by electron microprobe analysis (EPMA, Model JXA-8100, JEOL, Japan) and energy dispersive analysis system of X-ray (EDX, Model Link ISIS-300, Oxford, UK).

### 3. Results and discussion

The in-line transmittance and absorption spectrum of specimens A, B and C at room temperature are shown in Figs. 1 and 2. According to the Rayleigh's equation, the scattering intensity

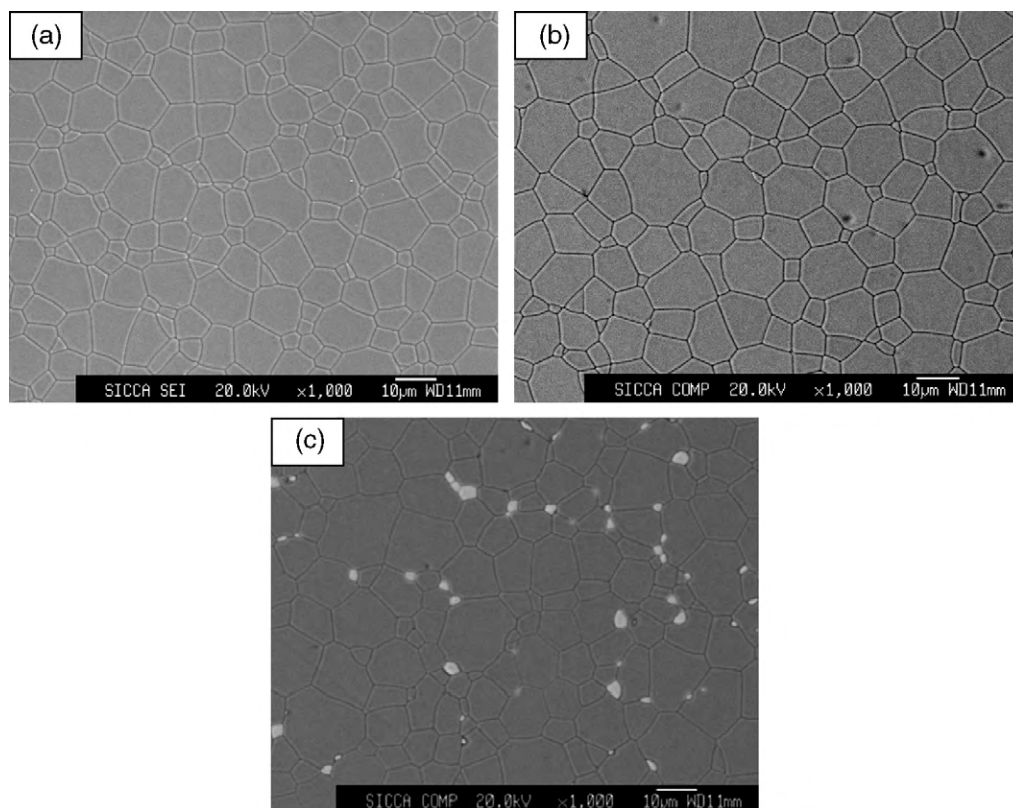


Fig. 3. EPMA micrographs of specimens A, B and C.

increases proportionally with  $\lambda^{-4}$ , where  $\lambda$  is the wavelength. So the scattering intensity increases with the decrease of wavelength [6]. The transmittances of the three specimens are all above 80% at lasing wavelength of 1064 nm, because the long wavelength is slightly affected by scattering centers when light passes through transparent ceramics. However, at the wavelength of 400 nm, the optical transmittance of the specimen A and specimen B were 82.45% and 81.35% respectively, that of specimen C was 77.89% because of the existence of scattering centers (pores and secondary phases) in the ceramics.

In order to detect the main reason for lower transmittance of specimen C at the wavelength of 400 nm, the phase compositions of the specimens are identified by XRD, as shown in Fig. 2. The diffraction peaks can be well indexed as the cubic garnet structure of  $\text{Y}_3\text{Al}_5\text{O}_{12}$  (YAG, JCPDS 88-2048), indicating that full transformation to YAG occurred, and the amount of secondary phases (YAM, YAP and so on) in the ceramics cannot be measured in the present study, but the reason for the fairly small amount of grain boundary phases in polycrystalline ceramics must be considered [11].

Fig. 3 displays the EPMA micrographs of the thermal etched surfaces of specimens A, B and C. It can be seen that the average grain sizes, pores and secondary phase amounts increased versus increasing the heating rate. That is because increase in the heating rate raises the rapid densification rate of the Nd:YAG ceramics, which obstructs pores exclusion and element diffusion. The specimen A has a fine microstructure (shown in Fig. 3(a)). The average grain size is about 10  $\mu\text{m}$ . There are no obvious pores and secondary phases in or between the grains. Fig. 3(b) shows the average grain size of specimen B is slightly larger than that of specimen A. there are a few pores observed both at the grain boundaries and inner grains, and no secondary phases. As can be seen in Fig. 3(c), many pores and secondary phases are found both along the grain boundaries and inner grains. The results of the present work indicate that the pores and secondary phases in Nd:YAG ceramic increase with increasing of heating rate. The optical transmittance of Nd:YAG ceramics is closely related to pores and secondary phases, light transmission is the main parameter for evaluating the optical properties of transparent ceramics, so the optical

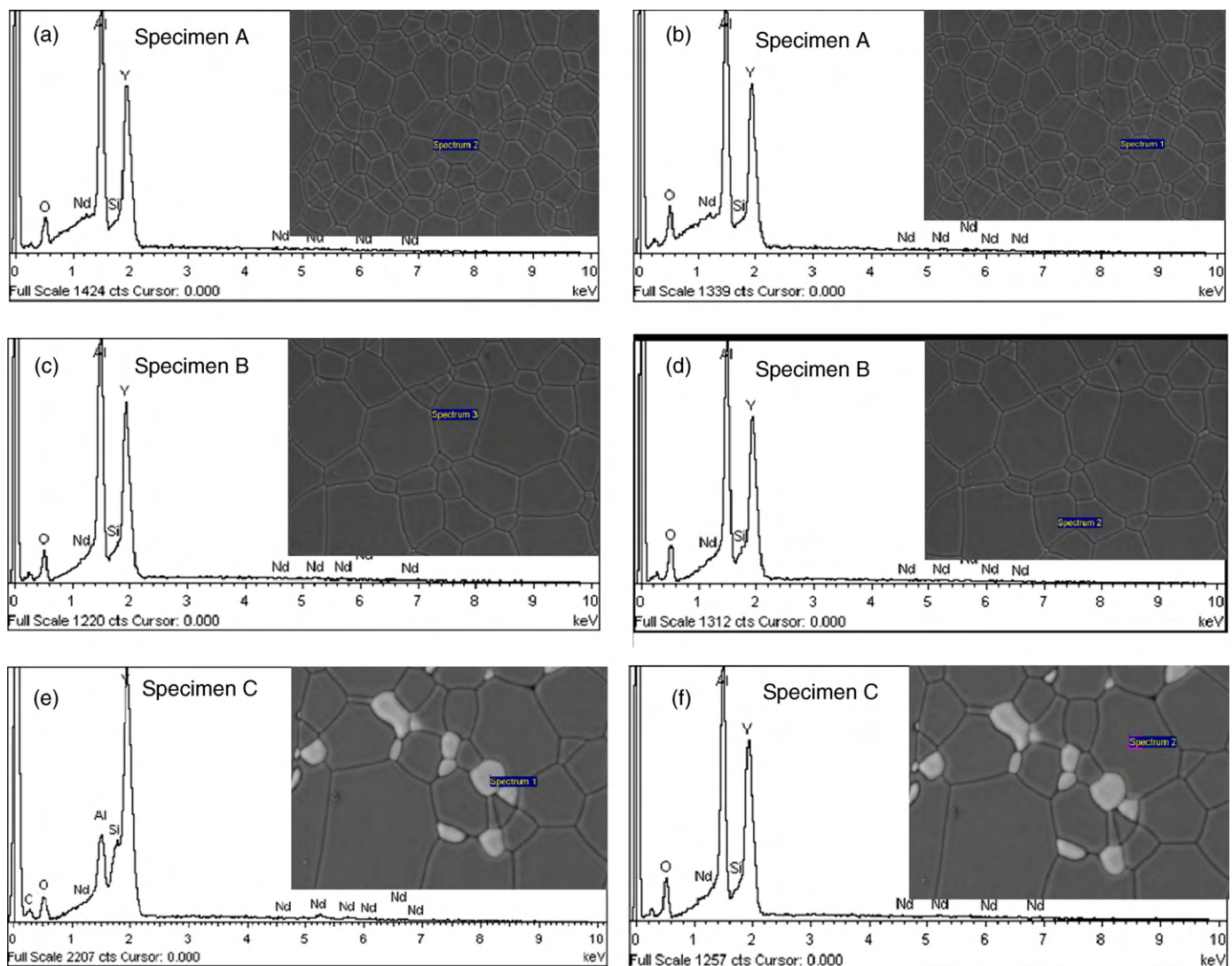


Fig. 4. EDX spectra analysis of specimens A, B and C.



Table 1  
Quantitative analysis of between and inner grains of specimens A, B and C.

Number	At%	Y	Al	Si	Nd	O
Specimen A	Grain boundary	15.83	23.12	0.56	0.20	60.14
	Inner grain	15.76	23.15	0.54	0.19	60.15
Specimen B	Grain boundary	15.89	23.29	0.55	0.15	60.10
	Inner grain	15.73	23.47	0.54	0.14	60.11
Specimen C	Grain boundary	23.24	10.63	0.74	0.24	60.88
	Inner grain	15.73	23.47	0.54	0.14	60.11

properties of specimen A are the most excellent among the three specimens because of its low scattering center contents.

Fig. 4 shows the EDX spectra analysis of the contents of Y, Al, Si and O ions in specimens A, B and C. As can be seen from Table 1, the atomic ratio of Y, Al and Nd of specimens A and B is almost equal at the grain boundaries and inner grains. No secondary phases can be detected. It is because that slow heating rate helps with element diffusion. However, with the increase of heating rate, specimen C is completely densified before sufficient element diffusion. Therefore, some secondary phases are formed between the grains (shown in Fig. 4(e) and (f)). This phenomenon suggests that secondary phases appear in the grain boundary of the Nd:YAG ceramics because of rapid heating rate in the sintering process. Because pores decrease and element diffusion both depend on grain growth, the rapid heating rate is apt to lead to abnormal growth of grains, and some pores appear in and between the grains in the ceramics. Meanwhile, the rapid heating rate enhances grain growth kinetics, decreases the grain boundary surface energy, and contributes to the proliferation of the Y ion and Si ion towards grain boundaries. As the grain growth rate is faster than the ions diffusion rate, which lead to the heterogeneous diffusion of the ions in the ceramics, numerous secondary phases occurred between grains. In conclusion, all this impurity phases and pores are the main cause for the decreased transmittance.

Fig. 5 shows the high-resolution TEM micrograph of the grain boundary of specimen A. It can be seen that the grain

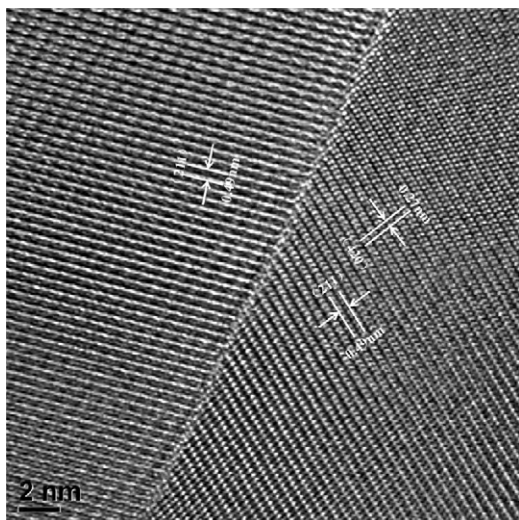


Fig. 5. HRTEM micrograph of the grain boundary of the specimen A.

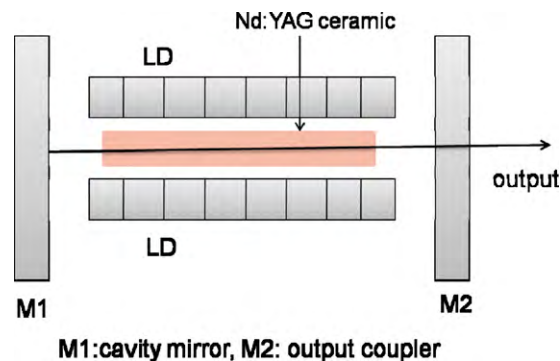


Fig. 6. Schematic diagram of the laser experimental setup.

boundary is clean and no extra grain boundary phase is present near the grain boundary. The interplanar spacing of the left grain is about 0.49 nm, which correspond to the distance between (2 1 1) planes of cubic YAG. The distance between (4 2 0) planes of the right YAG grain is about 0.268 nm. The width of YAG grain boundary is less than 1 nm. Then optical scattering caused by clean boundaries in Nd:YAG ceramics is insignificant which has been reported in previous papers [6,12].

Fig. 6 shows the schematic diagram of the laser experimental setup. A 140 W ring-shaped laser diode (LD) with the emission wavelength of 808 nm is used as pump source. The Nd:YAG ceramics are mirror polished on both surfaces and coated on the two parallel end facets. The laser cavity consists of two mirrors (M1 and M2), where input mirror (M1) is a flat high-reflection mirror at 1064 nm, and M2 was output mirror with transmittance of 5% at 1064 nm. The Nd:YAG ceramics are processed into the shape of  $\varnothing 3 \times 64 \text{ mm}^2$ .

Fig. 7 shows the laser output versus pump power for specimens A, B and C at 1064 nm. With 136 W of maximum absorbed pump power, laser output power of specimens A, B and C are 21.6 W, 16.8 W and 0.3 W respectively. The threshold for specimen A and specimen B are both 66 W which is 63 W lower than that of specimen C (129 W). The slope efficiency of specimen A is 30%, which is 6.67% higher than that of specimen B (23.33%). For the laser result of specimen C, the slope efficiency is 3% which is much less than that of specimen A and

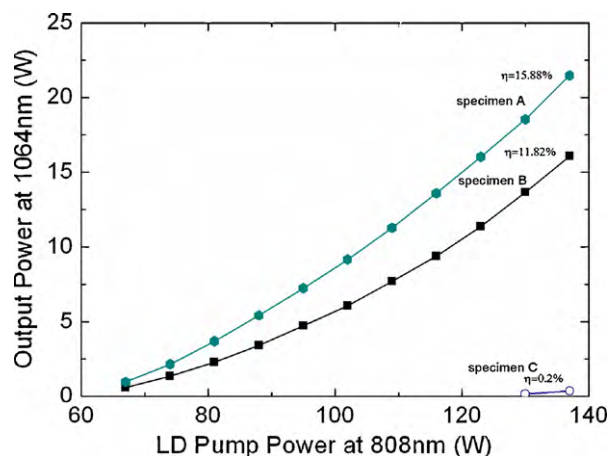


Fig. 7. Laser output at 1064 nm versus pump power.

B, and the main reason is that there are many scattering centers (mainly pores and secondary phases) in specimen C.

The laser results show that the quality of the Nd:YAG ceramics specimens is inferior to that of single crystal. This may be attribute to the scattering loss mainly caused by a very small quantity of residual pores in the three Nd:YAG ceramics. It is very important to decrease scattering centers to improve the optical properties of Nd:YAG ceramics. The detailed mechanism between the Nd:YAG ceramics sintering process and scattering loss need be studied further.

#### 4. Conclusion

The transparent ceramics of 0.8 at% Nd:YAG ceramics are fabricated with different heating rates in the sintering procedure. The structural and optical properties of the specimens are investigated. The average grain sizes and optical scattering centers (mainly pores or secondary phases) of specimens increase as the heating rate increases. The specimen A has a fine microstructure, with a uniform grain size of about 10  $\mu\text{m}$  and there are no pores and secondary phases in or between the grains. Clean grain boundaries in the specimen A cause decrease in optical centers or improvement of laser performance. The optical transmittances of specimens B and C are inferior to that of specimen A at the wavelength of 400 nm. The slope efficiencies (30%) and threshold (66 W) have been obtained for specimen A which is the best laser oscillation result in the three ceramics.

#### Acknowledgment

This work was supported by the Major Basic Research Program of NSFC (No. 50990300).

#### References

- [1] A. Ikesue, I. Furusato, K. Kamata, Fabrication of polycrystalline, transparent YAG ceramics by a solid-state reaction method, *J. Am. Ceram. Soc.* 78 (1) (1995) 225–228.
- [2] A. Ikesue, T. Kinoshita, K. Kamata, K. Yoshida, Fabrication and optical properties of high-performance polycrystalline Nd:YAG ceramics for solid-state lasers, *J. Am. Ceram. Soc.* 78 (4) (1995) 1033–1040.
- [3] J. Lu, M. Prabhu, J. Song, C. Li, J. Xu, K. Ueda, A.A. Kaminskii, H. Yagi, T. Yanagitani, Optical properties and highly efficient laser oscillation of Nd:YAG ceramics, *Appl. Phys. B* 71 (2000) 469–473.
- [4] T. Omatsu, T. Isogami, A. Minassian, M.J. Damzen, >100 kHz Q-switched operation in transversely diode-pumped ceramic Nd<sup>3+</sup>:YAG laser in bounce geometry, *Opt. Commun.* 249 (2005) 531–537.
- [5] H.X. Ma, Q.H. Lou, Y.F. Qi, J.X. Dong, Y.R. Wei, 5 W CW Yb<sup>3+</sup>:Y<sub>2</sub>O<sub>3</sub> ceramic laser pumped with 970 nm laser diode, *Opt. Commun.* 246 (2005) 465–469.
- [6] A. Ikesue, K. Kamata, T. Yamamoto, I. Yamaga, Optical scattering centers in polycrystalline Nd:YAG laser, *J. Am. Ceram. Soc.* 80 (6) (1997) 1517–1522.
- [7] J. Li, Y.S. Wu, Y.B. Pan, W.B. Liu, L.P. Huang, J.K. Guo, Fabrication, microstructure and properties of highly transparent Nd:YAG laser ceramics, *Opt. Mater.* 31 (2008) 6–17.
- [8] J. Li, Y.S. Wu, Y.B. Pan, H.M. Kou, Y. Shi, J.k. Guo, Densification and microstructure evolution of Cr<sup>4+</sup>,Nd<sup>3+</sup>:YAG transparent ceramics for self-Q-switched laser, *Ceram. Int.* 34 (2008) 1675–1679.
- [9] W.X. Zhang, Y.B. Pan, J. Zhou, W.B. Liu, J. Li, B.X. Jiang, X.J. Cheng, J.Q. Xu, Diode-pumped Tm:YAG ceramic laser, *J. Am. Ceram. Soc.* 92 (10) (2009) 2434–2437.
- [10] R. Boulesteix, A. Maitre, J.F. Baumard, C. Salle, Y. Rabinovitch, Mechanism of the liquid-phase sintering for Nd:YAG ceramics, *Opt. Mater.* 31 (2009) 711–715.
- [11] A. Ikesue, K. Kamata, Microstructure and optical properties of hot isostatically pressed Nd:YAG ceramics, *J. Am. Ceram. Soc.* 79 (7) (1996) 1923–1933.
- [12] A. Ikesue, K. Kamata, K. Yoshida, Synthesis of Nd<sup>3+</sup>,Cr<sup>3+</sup> co-doped YAG ceramics for high-efficiency solid-state lasers, *J. Am. Ceram. Soc.* 78 (9) (1996) 2545–2547.